Atomic Photoeffect in the Range $E_\gamma = 1$–2000 keV

G. RAKAVY AND A. RON*

Department of Theoretical Physics, The Hebrew University, Jerusalem, Israel

(Received 9 February 1967)

Photoelectric cross sections are presented for photon energies in the range 1–2000 keV. The atomic wave functions have been evaluated using Shalitin's modified Fermi–Amaldi potential, except for uranium, for which the Thomas-Fermi potential is used. The results are probably accurate to a few percent.

THIS paper reports on rather extensive and accurate numerical calculations of photoelectric cross sections in the energy range 1–2000 keV.[1] In the low-energy range and for heavy atoms the effect of atomic screening on the photoelectric cross sections is expected to be important. Besides, for the heaviest atoms relativistic effects are not negligible. In the relativistic domain only approximate expressions for the photoelectric cross sections are available.[2–4] These expressions are essentially expansions in $Z/137$ or in $(Z/137)\times(mc^2/E_\gamma)$ and are not expected to yield satisfactory results at intermediate energies and for heavy atoms. One has thus to resort to numerical calculations. With the aid of modern high-speed computers such calculations are quite feasible and several of them have been performed in recent years.[5–11] Here a rather complete compilation of total cross sections is presented. A tabulation of angular distributions and polarizations would be too voluminous.

TABLE I. Total cross sections in barns for the K and L subshells of uranium, $Z=92$ (calculated with a TF potential).

Photon energy (keV)	K	Subshell $L_{\rm I}$	$L_{\rm II}$	$L_{\rm III}$
2000	2.325	0.2854	0.0926	0.0415
1332	4.822	0.5856	0.1975	0.0908
1173	6.136	0.759	0.252	0.1187
662	19.74	2.438	0.8818	0.4496
412	58.02			
279	150.5	17.75	8.118	5.012
208	316.2	36.13	18.36	12.30
150	725.4			
130	1040			
120	1268			
116.5	1365			
103		194.9	135.8	112.2
81		339.4	269.1	239.3
60		661.2	626.8	610.5
42		1399	1672	1819
30		2692	4077	4941
22		4669	8895	12 030
21.5			9401	
20				15 720
17.5				22 670

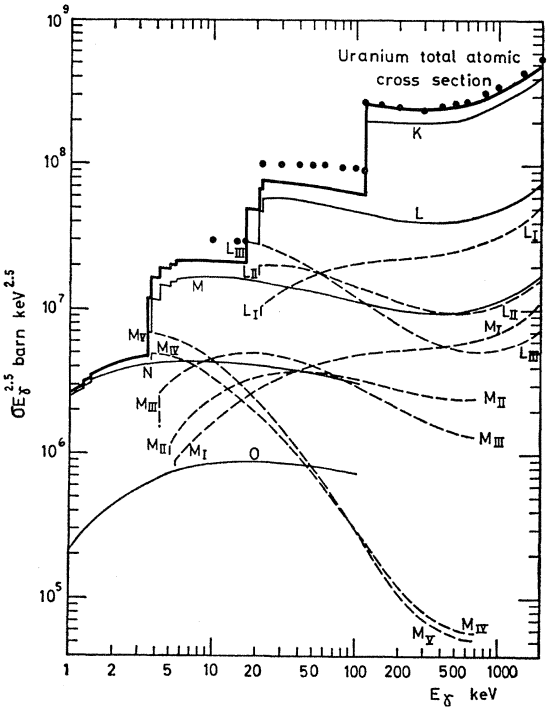

FIG. 1. Photoelectric cross sections of uranium ($Z=92$). The points are taken from Ref. 14.

* Present address: Department of Physics, University of Virginia, Charlottesville, Virginia.

[1] Most results for uranium were published by the authors in Phys. Letters **19**, 207 (1965). A full account on the calculations of the cross sections reported in the present work was given in Hebrew by A. Ron in his Ph.D. thesis for Hebrew University, Jerusalem, 1966 (unpublished).

[2] M. Gavrila, Phys. Rev. **113**, 514 (1959); **124**, 1132 (1961).

[3] R. H. Pratt, Phys. Rev. **117**, 1017 (1960); **119**, 1619 (1960).

[4] V. G. Gorshkov and A. I. Mikhailov, Zh. Eksperim. i Teor. Fiz. **43**, 991 (1962) [English transl.: Soviet Phys.—JETP **16**, 701 (1963)].

[5] S. Hultberg, B. Nagel, and P. Olsson, Arkiv Fysik **20**, 555 (1960).

[6] R. H. Pratt, R. D. Levee, R. L. Pexton, and W. Aron, Phys. Rev. **134**, A898 (1964).

[7] W. R. Alling and W. R. Johnson, Phys. Rev. **139**, A1050 (1965).

[8] J. J. Matese and W. R. Johnson, Phys. Rev. **140**, A1 (1965).

[9] H. Hall and E. C. Sullivan, Phys. Rev. **152**, 4 (1966).

[10] R. D. Schmickley and R. H. Pratt, thesis, Stanford University, 1966 (unpublished); Bull. Am. Phys. Soc. **12**, 68 (1966).

[11] S. Hultberg, B. Nagel, and P. Olsson (unpublished).

The expression for the photoelectric cross section is obtained by inserting into the general formula

$$d\sigma/d\Omega_e=[2\pi pE_e/(2\pi\hbar c)^3]V_{\rm norm}{}^2 \mid T_{fi}\mid^2 \quad (1)$$

the matrix element

$$T_{fi}=\left(\frac{2\pi e^2c^2\hbar}{\omega V_{\rm norm}}\right)^{1/2}\int \phi_f{}^{-*}(\mathbf{r}) \times \exp(ikz)\sigma_q\gamma_5\phi_i(\mathbf{r})\, d^3r, \quad q=\pm 1 \quad (2)$$

with the initial state[12]

$$\phi_i=\frac{1}{r}\begin{pmatrix} g_{l_ij_i}\chi_{l_ij_im_i} \\ if_{l_ij_i}\chi_{\bar{l}_ij_im_i}\end{pmatrix} \quad (3)$$

and the final state

$$\phi_f{}^-=(1/V_{\rm norm}{}^{1/2})[(E_e+mc^2)/2E_e]^{1/2}(4\pi/p_e)\sum_{ljm\mu} i^l \times \exp(-i\delta_{lj})(l\mu\,\tfrac{1}{2}\nu\mid jm)Y_{l\mu}{}^*(\Omega_e)\psi_{ljm}, \quad (4)$$

$$\psi_{ljm}=(1/r)\begin{pmatrix} g_{lj}(r)\chi_{ljm} \\ if_{lj}(r)\chi_{\bar{l}jm}\end{pmatrix}, \quad (5)$$

$$\chi_{ljm}=\sum_{\mu\nu}(l\mu\tfrac{1}{2}\nu\mid jm)Y_{l\mu}(\Omega)\chi_\nu. \quad (6)$$

Here,

$$s_z\chi_\nu=\nu\chi_\nu.$$

The functions f, g satisfy the radial Dirac equations. The bound states are normalized to

$$\int_0^\infty (g_{l_ij_i}{}^2+f_{l_ij_i}{}^2)\, dr=1 \quad (7)$$

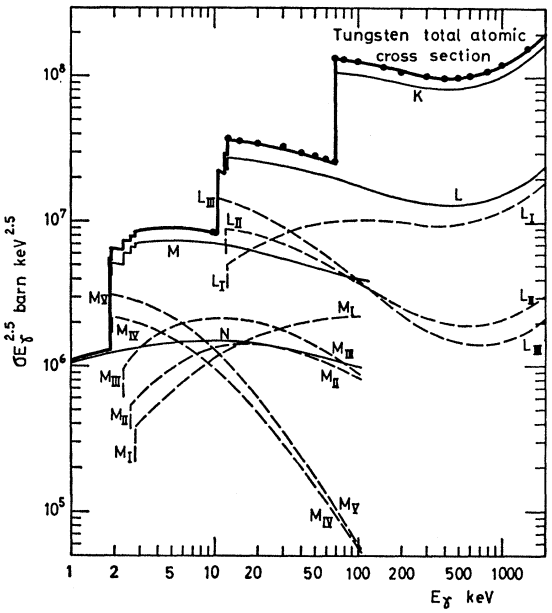

FIG. 2. Photoelectric cross sections of tungsten ($Z=74$). The points are taken from Ref. 14.

and the continuum states behave asymptotically as follows:

$$g_{lj}\to\sin(p_er-\tfrac{1}{2}(\pi l)+\delta_{lj}),$$
$$f_{lj}\to[\hbar cp_e/(E_e+mc^2)]^{1/2}\cos(p_er-\tfrac{1}{2}(\pi l)+\delta_{lj}). \quad (8)$$

Expanding the interaction in spherical harmonics, substituting expressions (3) and (4) for the wave functions, and performing all the summations over magnetic quantum numbers, the expression for the differential cross

TABLE II. Total cross sections in barns for M subshells of uranium, $Z=92$ (calculated with a TF potential).

Photon energy (keV)	Subshell $M_{\rm I}$	$M_{\rm II}$	$M_{\rm III}$	$M_{\rm IV}$	$M_{\rm V}$
2000	0.0647				
662	0.554	0.2185	0.1188	0.00496	0.00461
279	4.030				
208	8.198				
103	44.48	30.17	26.76	2.88	2.843
81	77.94	58.08	55.47	7.043	7.162
50	230.9	208.8	230.7	42.14	45.50
25	981.7	1151	1570	513.0	597.5
10	5182	7643	14 350	10 930	13 860
6	11 010	16 615			
5.5		18 425			
5			56 100	84 920	114 000
4				154 600	211 500

[12] M. E. Rose, *Relativistic Electron Theory* (John Wiley & Sons, Inc., New York, 1961).

TABLE III. Total cross sections in barns for N subshells of uranium, $Z=92$ (calculated with a TF potential).

Photon energy (keV)	Subshell N_{I}	N_{II}	N_{III}	N_{IV}	N_{V}
103	12.11	7.95	7.103	0.8394	0.8266
10	1616	2075	3683	2374	3013
5	5290	6863	15 420	15 300	20 570
3	11 430				
2	19 310	19 970	72 170	101 800	149 100
1.75		21 690			
1.5			106 000		
1				212 700	350 000

section can be cast into the form

$$d\sigma/d\Omega_e=(8\pi E_e/\alpha^{-1}p_e^2E_\gamma)[(E_e+mc^2)/2E_e]^{1/2}\sum_{n=0} B_nP_n(\cos\theta_e), \tag{9}$$

$$B_n=4p_e\sum_{L_1L_2}\sum_{\Lambda_1\Lambda_2}\sum_{l_1l_2}\sum_{j_1j_2}(-1)^{j_i-1/2+L_1+L_2+j_1+j_2i l_2-l_1+\Lambda_1-\Lambda_2}$$
$$\times\exp[i(\delta_{l_1j_1}-\delta_{l_2j_2})][(2\Lambda_1+1)(2\Lambda_2+1)(2l_1+1)(2l_2+1)(2j_1+1)(2j_2+1)]^{1/2}$$
$$\times(l_10l_20\mid n0)(\Lambda_101q\mid L_1q)(\Lambda_201q\mid L_2q)(L_1qL_2-q\mid n0)W(l_1l_2j_1j_2;n\tfrac{1}{2})$$
$$\times W(L_1L_2j_1j_2;nj_i)(\psi_{l_ij_i}\|j_{\Lambda_1}S_{\Lambda_1L_1\gamma_1}\|\phi_i)(\psi_{l_2j_2}\|j_{\Lambda_2}S_{\Lambda_2L_2\gamma_1}\|\phi_i)^*. \tag{10}$$

The cross sections for circularly polarized photons are the same as for unpolarized photons; thus in expression (10) q can be chosen $+1$ or -1. We obtain the simpler form

$$\sigma=\frac{32\pi^2}{\alpha^{-1}}\frac{1}{p_e^2}\frac{E_e}{E_\gamma}\left[\frac{(E_e+mc^2)}{2E_e}\right]^{1/2}B_0 \tag{11}$$

for the total cross section, where

$$B_0=4p_e\sum_L\sum_l\sum_j\{|(\psi_{lj}\|j_LS_{L,L\gamma_5}\|\phi_i)|^2+[L/(2L+1)]\,|(\psi_{lj}\|j_{L+1}S_{L+1,L\gamma_5}\|\phi_i)|^2$$
$$+[(L+1)/(2L+1)]\,|(\psi_{lj}\|j_{L-1}S_{L-1,L\gamma_5}\|\phi_i)|^2-|[2(L(L+1))^{1/2}/(2L+1)]$$
$$\times\{\mathrm{Re}\{(\psi_{lj}\|j_{L+1}S_{L+1,L\gamma_5}\|\phi_i)(\psi_{lj}\|j_{L-1}S_{L-1,L\gamma_5}\|\phi_i)^*\}\}. \tag{12}$$

The reduced matrix elements appearing here are

$$(\psi_{lj}\|j_\Lambda S_{\Lambda L\gamma_5}\|\phi_i)=i(\bar{l}j\|S_{\Lambda L}\|l_ij_i)\int_0^\infty g_{l_ij_i}(r)j_\Lambda(kr)f_{lj}(r)\,dr$$
$$-i(lj\|S_{\Lambda L}\|\bar{l}_ij_i)\int_0^\infty f_{\bar{l}_ij_i}(r)j_\Lambda(kr)g_{lj}(r)\,dr, \tag{13}$$

$$(l_1j_1\|S_{\Lambda L}\|l_2j_2)=[(2j_1+1)(2j_2+1)(2L+1)]^{1/2}(l_1\|Y_\Lambda\|l_2)(\tfrac{1}{2}\|s\|\tfrac{1}{2})X\begin{pmatrix}\Lambda & 1 & L\\ l_1 & \frac{1}{2} & j_1\\ l_2 & \frac{1}{2} & j_2\end{pmatrix}$$
$$=(-)^{l_2}[(2j_1+1)(2j_2+1)(2l_1+1)(2l_2+1)(2L+1)\times 3/8\pi]^{1/2}(l_10l_20\mid\Lambda0)X\begin{pmatrix}\Lambda & 1 & L\\ l_1 & \frac{1}{2} & j_1\\ l_2 & \frac{1}{2} & j_2\end{pmatrix}. \tag{14}$$

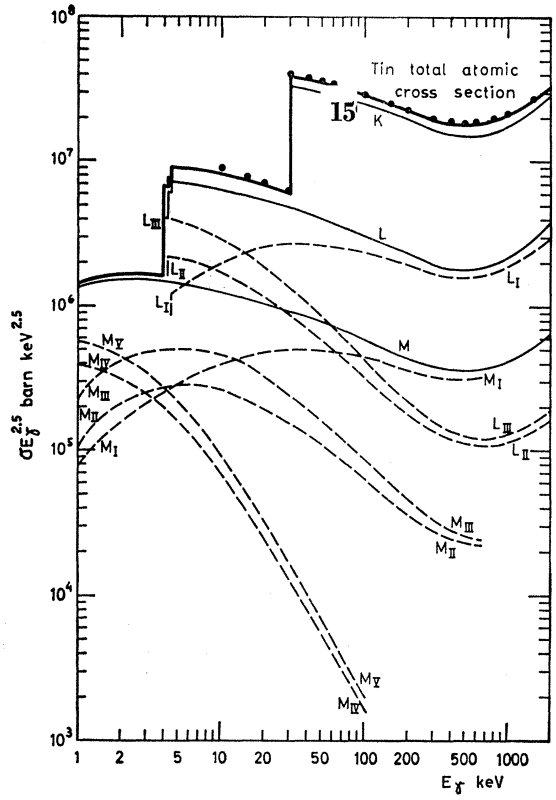

FIG. 3. Photoelectric cross sections of tin ($Z=50$). The points are taken from Ref. 14.

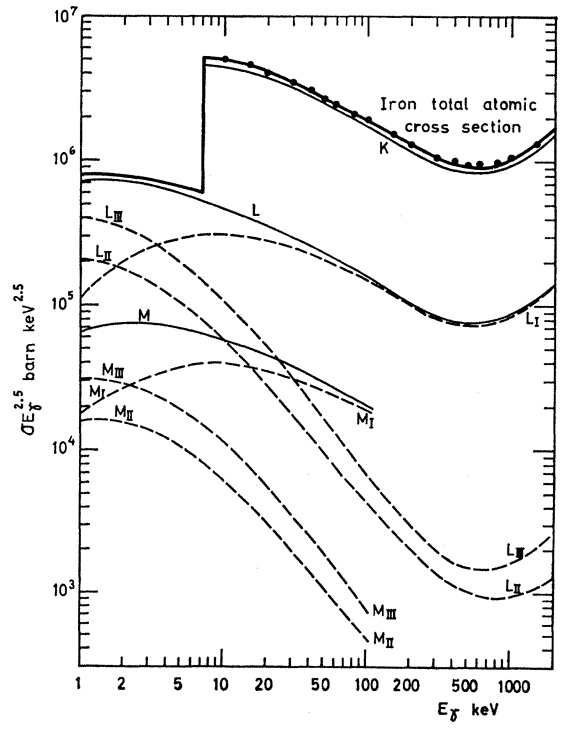

FIG. 4. Photoelectric cross sections of iron ($Z=26$). The points are taken from Ref. 14.

TABLE IV. Total cross sections in barns for N and O subshells of uranium, $Z=92$ (calculated with a TF potential).

Subshell	Photon energy (keV) 103	10	5	3	1
N_{VI}	0.01515	418.3	5933	125 500	801 800
N_{VII}	0.01564	501.1	7281	158 500	1 037 000
O_I	3.096	427.8	1472	6472	17 040
O_{II}	1.896	499.7	1735	6466	13 390
O_{III}	1.636	842.9	3595	18 540	52 180
O_{IV}	0.1599	427.8	2703	18 640	50 880
O_V	0.1544	532.5	3558	26 400	77 110

TABLE V. Total cross sections in barns for K and L subshells of tungsten, $Z=74$ (calculated with FAM potentials).

Photon energy (keV)	Subshell K	L_I	L_{II}	L_{III}
2000	0.9168	0.1054	0.01722	0.01216
1173	2.399	0.2771	0.04707	
662	7.911	0.9126	0.1703	0.1257
279	66.66	7.378	1.742	1.445
103	964.2	95.41	35.14	35.99
81	1803.5	173.6	73.51	79.28
71	2536			
50		549.8	319.4	380.5
30		1712	1450	1909
15		6732	10 030	15 110
12.75		8942		
12.2			17 170	
11				35 920

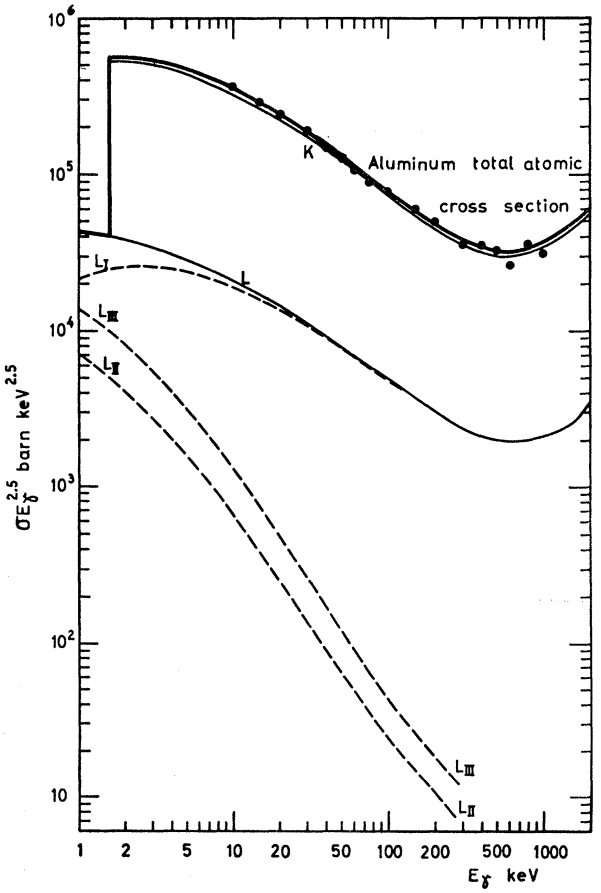

FIG. 5. Photoelectric cross sections of aluminium ($Z=13$). The points are taken from Ref. 14.

TABLE VI. Total cross sections in barns for M subshells of tungsten, $Z=74$ (calculated with FAM potentials).

Photon energy (keV)	Subshell M_{I}	M_{II}	M_{III}	M_{IV}	M_{V}
103	20.48	7.215	8.719	0.4920	0.5287
81	37.27	15.81	17.73	1.256	1.381
50	119.0	65.04	80.60	8.260	9.558
30	380.3	273.0	373.8	58.86	71.18
10	3605	4266	7153	3123	4083
5	12 200	17 320	33 800	29 560	40 140
3.5	20 980	31 020			
3			88 060		
2.5				214 200	302 500

TABLE VII. Total cross sections in barns for N subshells of tungsten, $Z=74$ (calculated with FAM potentials).

Photon energy (keV)	Subshell N_{I}	N_{II}	N_{III}	N_{IV}	N_{V}
103	5.012	1.812	1.921	0.1177	0.1255
81	9.123	3.696	4.127	0.2977	0.3260
50	29.20	15.06	18.59	1.917	2.203
30	93.92	62.55	85.20	13.23	15.94
10	930.7	966.9	1596	618.0	805.8
5	3422	4123	7693	5075	6894
1	41 550	42 760	121 200	170 900	254 400

TABLE VIII. Total cross sections in barns for N and O subshells of tungsten, $Z=74$ (calculated with FAM potentials).

Photon energy (keV)	Subshell N_{VI}	N_{VII}	O_{I}	O_{II}	O_{III}
5	701.8	873.1	707.7	718.0	1261.
1	188 100	242 100	10 580	9248	22 660

TABLE IX. Total cross sections in barns for K and L subshells of tin, $Z=50$ (calculated with FAM potentials).

Photon energy (keV)	Subshell K	L_{I}	L_{II}	L_{III}
2000	0.1635	0.01718	0.0009111	0.001108
1173	0.4207	0.04432	0.002565	0.002934
662	1.416	0.1490	0.009764	0.01071
279	13.24	1.358	0.1140	0.1308
103	229.3	21.76	2.924	3.884
81	455.2	42.05	6.557	8.923
40	3168	269.6	69.62	102.9
30	6683	551.8	179.0	273.4
10		6533	5494	9292
5		23 910	38 640	69 100
4.5			50 890	
4.25				107 900

TABLE X. Total cross sections in barns for M subshells of tin, $Z=50$ (calculated with FAM potentials).

Photon energy (keV)	Subshell M_{I}	M_{II}	M_{III}	M_{IV}	M_{V}
662	0.02847	0.001987	0.002214		
279	0.2588	0.02302	0.02655		
103	4.113	0.5746	0.7634	0.01475	0.01752
81	7.929	1.275	1.752	0.03982	0.04901
40	50.63	12.94	19.42	0.7770	0.9952
30	103.8	32.45	50.22	2.587	3.365
10	1287	850.4	1455	210.9	288.7
5	5273	5143	9297	2702	3788
3	13 660	16 450	31 090	15 370	21 880
1	75 360	106 600	230 600	391 300	571 500

TABLE XI. Total cross sections in barns for N subshells of tin, $Z=50$ (calculated with FAM potential).

Photon energy (keV)	Subshell N_{I}	N_{II}	N_{III}	Photon energy (keV)	Subshell N_{I}	N_{II}	N_{III}
103	0.7552			10	238.3		
81	1.455			5	997.3	801.8	1424
40	9.287			3	2664	2581	4762
30	19.04			1	18 200	20 080	40 480

TABLE XII. Total cross sections in barns for K and L subshells of iron, $Z=26$ (calculated with FAM potentials).

Photon energy (keV)	Subshell K	L_{I}	L_{II}	L_{III}
2000	0.008414	0.0007505	0.000007201	0.00001441
1173	0.02116	0.001890	0.00002072	0.0000367
662	0.07196	0.006419	0.00008249	0.0001253
279	0.7388	0.06531	0.001109	0.001625
120	9.574			
103	15.34	1.315	0.03706	0.05924
81	32.12	2.721	0.08989	0.1466
30	639.3	50.26	3.577	6.297
10	13 940	964.3	182.4	334.6
7.65	27 600			
5		5113	1856	3483
3		15 630	9272	17 640
1		112 450	203 900	400 400

TABLE XIII. Total cross sections in barns for M subshells of iron, $Z=26$ (calculated with FAM potentials).

Photon energy (keV)	Subshell M_{I}	M_{II}	M_{III}	Photon energy (keV)	Subshell M_{I}	M_{II}	M_{III}
103	0.168	0.00416	0.006649	5	648.4	185.6	347.5
81	0.3472	0.01011	0.01643	3	2014	870.7	1650
30	6.375	0.3953	0.6927	1	17 570	15 770	30 590
10	121.6	19.28	35.42				

TABLE XIV. Total cross sections in barns for K and L subshells of aluminum, $Z=13$ (calculated with FAM potentials).

Photon energy (keV)	Subshell K	L_I	L_{II}	L_{III}
2000	0.0003185			
662	0.002692			
279	0.0291	0.001894	0.000005535	0.000009354
103	0.6765	0.04382	0.0002101	0.0003775
81	1.468	0.09491	0.00053	0.0009589
30	35.19	2.205	0.02736	0.0516
10	1036	60.80	2.051	3.928
5	7862	430.2	27.96	54.65
3		1644	178.0	346.4
2	93 645			
1		22 750	7152	14 070

According to Shalitin's analysis of binding energies[13] a modified Fermi–Amaldi potential (denoted FAM) gives very good results for atoms with Z below 50. For very high Z the conventional Thomas-Fermi potential (denoted TF) gives satisfactory results. The errors in the binding energies are only of a few percent and are, on the average, not larger than the ones inherent in results obtained with Hartree–Fock self-consistent field potentials. In our calculations it was decided to use the FAM potentials for all atoms except for uranium. For the latter the TF potential was used. In the intermediate region (Z between 50 and 80) it was found that the difference in cross sections obtained by using FAM and TF potentials is less than 1.5%. The difference is larger for Z below 50, but in all cases which we checked it did not exceed 5%. It was also found that for the K shell the screening of the Coulomb field is negligible, but for all higher shells screening effects are important.

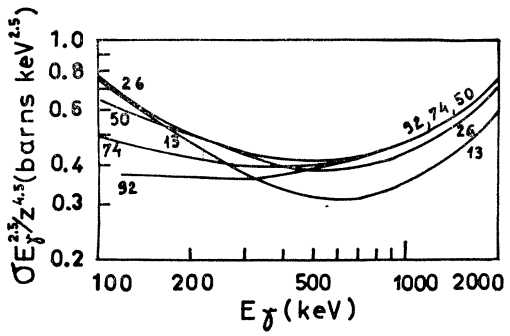

FIG 6. Total atomic cross sections of various elements at intermediate photon energies. The numbers on the curves designate the Z of the element. Notice that the cross sections vary roughly as $Z^{4.5}/E^{2.5}$.

Comprehensive checks, including comparison with numerical results of Refs. 5–11, show that the numerical accuracy of the calculations is better than 0.5%. Uncertainties in the cross sections resulting from the use of an inaccurate effective central potential are not believed to be more than a few percent.

The results of the calculations are presented in Tables I–XIV and in Figs. 1–5.[14] In Fig. 6 the atomic cross sections above 100 keV are summarized in a convenient form.

It is a pleasure to thank Dan Shalitin for generous help and advice through many phases of our work.

[13] D. Shalitin, Phys. Rev. **140**, A1857 (1965).

[14] C. M. Davisson, in *Alpha-, Beta-, and Gamma-Ray Spectroscopy*, edited by K. Siegbahn (North-Holland Publishing Company, Amsterdam, 1965), Vo . 1.